Optimization of Superplastic Forming; Effects of Interfacial Friction on Variable Strain Rate Forming Paths

M.I. Albakri, M.K. Khraisheh

Masdar Institute of Science and Technology, Abu Dhabi, UAE

Abstract

Superplastic forming technique provides a unique solution for meeting the growing demand on light-weight materials for transportation applications. However, being a rate controlled process, confined to low strain rates, makes it relatively slow and unfavorable for mass production applications. In this paper, an optimal variable strain rate forming path based on a multi-scale stability criterion is developed, aiming at reducing forming time while maintaining the integrity of the formed parts. This criterion accounts for geometrical instabilities as well as microstructural features. The effects of friction distribution at the die-sheet interface on the deformation stability are also investigated; aiming at identifying the optimal lubrication conditions. These results are demonstrated through finite element simulations of the forming process of bipolar plates flow-field channels used for polymer electrolyte membrane fuel cells.

Keywords

Bipolar Plates; Interfacial Friction; Lightweight Alloys; PEM Fuel Cells; Superplastic Forming; Variable Strain Rate.

1 INTRODUCTION

Environmental issues; global warming and climate change in particular, have been attracting more attention in the last few years. Countries all over the world are requested to cut down their greenhouse gas (GHG) emissions, especially CO_2, in order to meet the international standards. In most of the developed countries, transportation sector has always been a major source of GHG emissions, contributing to about 29% of the total emissions in the European Union and United States [1]. With the growing environmental awareness, these numbers have become a source of a continuously growing pressure on transportation industry, the automotive in particular, to reduce fuel consumption along with the levels of exhaust gas emissions.

To achieve the required emissions reduction, cutting down the mass of the vehicles is one of the most influential and least costly methods. However, customers' increasing demand for safer, more powerful and luxurious vehicles has been adding more weight to the various components of the vehicles, making the realization of lighter cars more difficult and challenging [2]. Thus, the targeted weight reduction will not be feasible on the desired scales without the extensive use of light yet strong-enough materials.

In addition to introducing lighter vehicles, exhaust emissions can be significantly reduced by introducing new, clean and renewable power sources to replace the conventional internal combustion engines. Among the different sources available, fuel cells, proton exchange membrane fuel cells (PEMFC) in particular, are the primary candidates for transportation applications. PEMFCs provide a promising, clean, and efficient energy solution. However, a number of critical issues such as cost, size, weight, and overall efficiency have to be addressed for the widespread use of PEMFCs.

PEMFC consists of three main components; the membrane electrode assembly (MEA), the gas diffusion layer (GDL), and the bipolar plates. Among these different parts, the bipolar plates account for more than 80% of the weight, more than 40% of the cost and occupy a large portion of the volume of the fuel cell [3]. Therefore, introducing new designs and technologies aiming at improving the performance of the bipolar plates and reducing their weight, size and cost are very much needed.

With their low densities, lightweight materials (LWM), such as titanium, aluminium and magnesium alloys are considered as a key solution towards achieving the desired weight reduction. These alloys are generally 43–78% lighter than conventional steels [2]; a fact accentuating the great weight-saving potentials promised by these materials. Unfortunately, due to their limited formability, the use of LWM for transportation applications is pretty much limited. However, several lightweight alloys exhibit extraordinarily enhanced ductility at elevated temperatures; a phenomenon known as superplasticity. This phenomenon has gained a lot of interest over the past few decades, and was put into practice to form several products out of these alloys by means of the Superplastic Forming (SPF) technique [4].

SPF is a near net shape forming process that offers many advantages over conventional forming operations including weight reduction, greater design flexibility, and the ability to form hard-to-form metals into complex shapes. However, low production rate and the non-uniformity of the formed parts are the main obstacles hindering the widespread use of SPF.

To overcome these problems, several studies have been published investigating the possibility of speeding up the forming process by designing variable strain rate forming paths based on different stability criteria [5-7]. Despite of their success, the reduction in forming time achieved with these methods has always been constrained by localized thinning taking place at certain areas of the sheet. Moreover, all of the stability criteria currently available do not account for the

G. Seliger et al. (eds.), *Advances in Sustainable Manufacturing: Proceedings of the 8th Global Conference on Sustainable Manufacturing*, DOI 10.1007/978-3-642-20183-7_18, © Springer-Verlag Berlin Heidelberg 2011

effects of frictional forces acting at the die sheet interface. Such forces were found to have crucial effects on the way the metal flows during the forming process [8].

In this paper an optimal variable strain rate forming path based on a multi-scale stability criterion is developed, aiming at reducing forming time while maintaining the integrity of the formed parts. First, a microstructural based constitutive material model that describes the superplastic behavior of the 5083 fine-grained superplastic aluminum alloy is discussed. A multi-scale stability criterion is then developed, and based on it, a variable strain rate forming path is designed. This criterion accounts for geometrical instabilities as well as microstructural features. Moreover, the effects of friction distribution at the die-sheet interface on deformation stability are addressed through a number of FE simulations.

2 MATERIAL CONSTITUTIVE MODEL

A general constitutive model based on the continuum theory of viscoplasticity has been previously applied in modeling different superplastic materials including Al, Mg and Cu alloys [5],[9],[10]. A Similar model is used in this work to describe the superplastic behavior of fine grain AA5083 sheet at 450°C. This model accounts for microstructural features including grain growth and cavitation evolution, as given by the following equation:

$$\dot{\bar{\varepsilon}} = \frac{K}{d^{P}}\left(\frac{\bar{\sigma}}{1-f_a}\right)^{1/m} \tag{1}$$

where $(\dot{\bar{\varepsilon}})$ is the effective strain rate, ($\bar{\sigma}$) is the effective flow stress, (m) is the strain rate sensitivity index, (d) is the average grain size, (P) is the grain growth exponent, (f_a) is the area fraction of voids, and (K) is a material parameter defined as a function of the effective strain rate.

To account for the change in microstructure during deformation, evolution equations for grain size (d) and area fraction of voids (f_a) are used. For the former, a simple linear grain growth model similar to that Suggested by Caceres and Wilkinson[11] is used here, as given by Eq.2:

$$d = d_0 + c\bar{\varepsilon} \tag{2}$$

Where ($\bar{\varepsilon}$) is the effective strain, (d_0) is initial grain size, and (c) is a material constant.

Due to the large deformation associated with superplastic forming, cavitation is primarily controlled by the plastic flow of the surrounding matrix [12]. Such plasticity controlled growth of non-interacting cavities is described by the following equation:

$$f_a = f_{a0}\exp(\psi\bar{\varepsilon}) \tag{3}$$

Where (f_{a0}) is the initial area fraction of voids, and (ψ) is the void growth parameter. A fitting process is used to obtain the values of the different parameters for AA5083 material model, see table (1). In the resulting single-term phenomenological strain rate ($\dot{\bar{\varepsilon}}$), and thus (*m*) is only equal to the strain rate sensitivity at the start of deformation (i.e. $\bar{\varepsilon} = 0$). This model has proved to be capable of predicting the deformation behavior of this superplastic alloy under different loading conditions.

Table 1: Values of the material parameters [9]

Parameter	Value
m	0.5
P	$-3 - 0.43\ln(\dot{\bar{\varepsilon}})$
ln(K)	$-15.251 - 0.202\ln(\dot{\bar{\varepsilon}}) + 0.0346\ln^2(\dot{\bar{\varepsilon}})$
d_0	8.0
c	2.5
f_{a0}	1.25%
ψ	1.5

3 STABILITY ANALYSIS

To design an optimal variable-strain-rate forming path, the effective strain at which the onset of instability takes place needs to be determined as a function of the forming strain rate. To do so, deformation stability of the long cylindrical bar shown in Figure 1 is analyzed. This part contains a local non-uniform region where necking is more likely to occur. The one dimensional modified version of Marciniak and Kuczynski analysis [13], introduced by Hutchinson and Neale [14], is applied here. This stability criterion is coupled with the constitutive model described in the previous section so as to account for the effects of microstructural evolution on the deformation stability. The true stress and strain are defined using the true load bearing area reduced by cavitation. The initial fraction of non-uniformity is defined as:

$$\eta = \frac{A_u^0\left(1-f_{a,u}^0\right) - A_n^0\left(1-f_{a,n}^0\right)}{A_u^0\left(1-f_{a,u}^0\right)} \tag{4}$$

Where (A^0) and $\left(f^0_{\$\$a}\right)$ are the initial cross sectional area and the initial area fraction of voids, respectively. The subscripts (u) and (n) stand for the uniform and non-uniform regions, respectively.

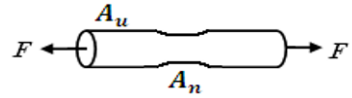

Figure 1: A long cylindrical bar containing a geometric non-uniformity and subjected to a time varying load.

Applying the nonlinear long-wavelength stability analysis, the following equation is obtained:

$$\bar{\sigma}_n e^{\bar{\varepsilon}_n} = \bar{\sigma}_u e^{\bar{\varepsilon}_u}\frac{1}{1-\eta} \tag{5}$$

Combining the constitutive material model (Equations 1-3) into Eq. 5, a relation between the increments of strain in the local non-uniform and uniform regions is obtained as follows:

$$\left(\frac{\dot{\bar{\varepsilon}}_n d^P}{k}\right)^m (1-f_{a,n})e^{-\bar{\varepsilon}_n} = \left(\frac{\dot{\bar{\varepsilon}}_u d^P}{k}\right)^m \frac{(1-f_{a,u})}{1-\eta}e \tag{6}$$

This equation is numerically integrated to calculate the strain ratio between the non-uniform and uniform sections as shown in Figure 2. Instability can be defined as the point at which the slope of the strain ratio curve approaches infinity. At this point, deformation will be localized in the non-uniform region, leading to necking and failure there. A more conservative approach can be adopted to design the variable strain rate forming path by defining a certain value of the strain ratio at which the deformation is considered to be unstable. In this study, a strain ratio of 1.5 is selected to define the critical strain for each forming strain rate shown in Figure 2. These critical-strain, strain-rate pairs form the basis for constructing the optimal variable strain rate paths that are used in the upcoming sections.

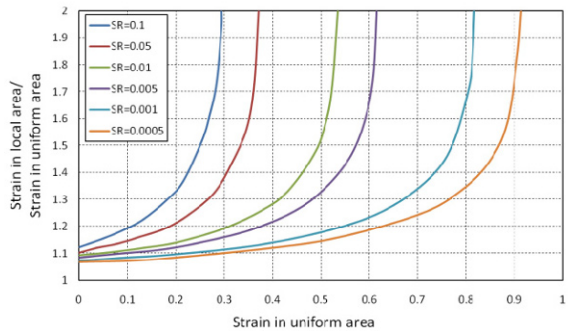

Figure 2: Ratio of strain in local area to the strain in uniform area as a function of strain in uniform area for different strain rates.

4 FINITE ELEMENT MODEL

The forming process of AA5083 sheet into PEMFC bipolar plate is addressed here. This bipolar plate has a serpentine flow field; as shown in Figure 3.a, with the dimensions given in Table 2. Based on a previous study, these dimensions were found to facilitate reactants mass transfer between the bipolar plate's flow field and the adjacent GDL resulting in an enhanced cell performance [15]. For such long channels, a state of plane strain exists in most of the part. This allows simplifying the simulation domain to a two-dimensional geometry by selecting only a section along the minor axis of the flow channel. Due to the shape symmetry only one half of the 2D version of the channel cross section is modeled, as shown in Figure 3.b.

The die is modeled as an analytical rigid surface which allows a better approximation to the physical contact constraints. This is due to the smoother surface description that results from the ability of analytical rigid surfaces to parameterize the surface with curved line segments [16]. On the other hand, the sheet is modeled using four layers of solid plane strain

Table 2: Channel geometry of the bipolar plate flow field

Parameter	Value(mm)
Channel Width	1.5
Channel Height	1
Land Width	1
Entry Radius	0.25
Bottom Radius	0.25

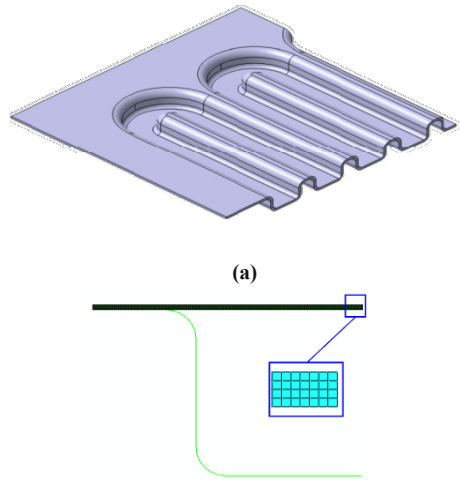

Figure 3: (a) Section through a serpentine flow field of a PEMFC bipolar plate (b) 2D FE model of the flow channel cross-section showing the layered plane strain elements of the sheet.

quadrilateral elements, with 300 elements in each layer. According to Luckey et al. [17], two-dimensional modeling using layered solid elements is more effective in predicting thinning behavior than three-dimensional modeling with conventional shell and membrane elements.

Frictional forces at the die sheet interface have been defined using the coulomb friction model available in ABAQUS^{TM}. With this model, the critical shear stress (τ_{ert}); which is the stress at which sliding between contacting surfaces occurs, is determined by the friction coefficient and the contact pressure, as given by the following equation:

$$\tau_{ert} = \mu.P \tag{7}$$

In blow forming practices, the contact pressure between the die and the sheet surfaces is just the same as the forming pressure applied on the top of the sheet. For all simulations, this forming pressure is controlled so as to maintain a target effective strain rate of 0.01 s^{-1} during the forming process. The averaging algorithm "5-20-75" described by [17],[18] is applied here. With this algorithm, the average of the lower 20% of the top 25% effective stresses found in the sheet is calculated in each step. Using this value, denoted by $\left(\bar{\sigma}^{t}_{20\%}\right)$, the forming pressure is adjusted according to the following equation:

$$P_{t+\Delta t} = \left(\frac{\bar{\sigma}_{tar}}{\bar{\sigma}^{t}_{20\%}}\right) P_t \tag{8}$$

Where ($\bar{\sigma}_{tar}$) represents the effective stress corresponding to the target strain rate, (P_t) and ($P_{t+\Delta t}$) are the values of the forming pressure at the current and next time increments, respectively.

5 RESULTS AND DISCUSSION

The commercial finite element code, ABAQUS™, is used to carry out the simulations. Three user defined subroutines are developed to define the material viscoplastic behavior and the forming pressure control algorithm. To study the effect of the interfacial friction distribution on the forming process, a homogeneous friction at the die-sheet interface is applied. For the same channel geometry and forming conditions, the coefficient of friction acting at the die-sheet interface is varied from a frictionless condition to 0.5; representing different lubrication conditions. Formed sheet thickness distribution, forming time and forming pressure profile are calculated for each case. This allows the identification of the optimal lubrication conditions for this geometry.

5.1 Frictional Effects on SPF

The effect of the friction coefficient on the formed sheet thickness profile is shown in Figure 4. With excessive lubrication, represented by low friction coefficients, a localized thinning was found to take place at the die entry region. This excessive thinning occurs due to the combined compression and bending acting on this region during the initial stages of the forming process. Furthermore, such localized straining boosts the voids area fraction, given by eq. 3, compromising the load bearing capacity of the die entry region and making it weaker than the rest of the sheet. With small values of interfacial friction coefficients, metal will keep flowing from this weak area, and at later stages of the forming process, this strain peak becomes substantially large and may result in premature failure. On the other hand, with higher friction coefficients, less material is allowed to flow once it gets in contact with the die. This will enhance the deformation stability at the die entry region, and reduce thinning there. However, with such high friction, more thinning is found to take place at the die bottom corner, as it is the last part of the sheet that gets in contact with the die. The thinning taking place at this area doesn't indicate instability, as no strain localization is noticed and the strain is uniformly distributed over the die bottom corner. The friction coefficient at which the location of the minimal thickness moves from the die entry region to the bottom corner represents the optimal case, where the least localized thinning at both regions is obtained. This value will be referred to as the optimal homogeneous friction coefficient, and from Figure 4, it could be noticed that for the channel geometry addressed here, this optimal value is about 0.4.

The shape of the forming pressure profile, shown in Figure 5, is governed by changes in sheet thickness, sheet's radius of curvature, forming strain rate, the die-sheet interaction in addition to the coefficient of friction. During the early stages in the forming process, the pressure required to maintain the target strain rate increases as the rate of change of the sheet's radius of curvature is much higher than the rate of change of its thickness. Thus, higher pressure is required to maintain the target strain rate. However, as the forming process proceeds, the thickness reduction rate increases and the area fraction of voids becomes more significant, causing a slight reduction in the forming pressure. This applies until the

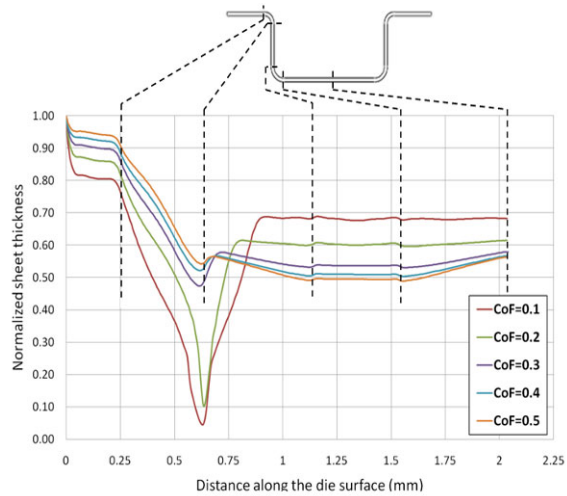

Figure 4: Predicted thickness profile of the formed sheet with different values of friction coefficient

sheet gets in contact with the base of the die. Once that happens, the rate of change of the radius dominates again, resulting in a rapid increase in the forming pressure.

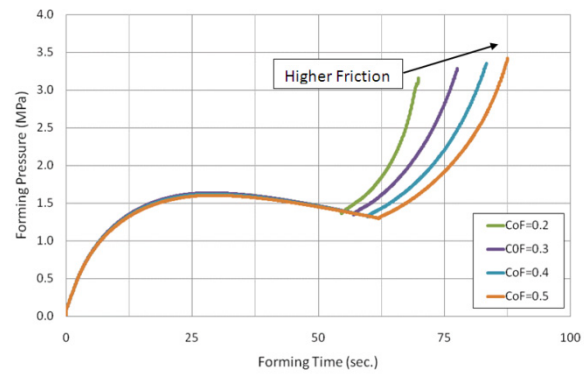

Figure 5: Forming pressure profile with different values of friction coefficient for target strain rate of 0.01 s-1

The previously described trend in the forming pressure profile remains valid regardless the value of the interfacial friction. In the first stage of the forming process, i.e. before the sheets gets in contact with the bottom surface of the die, frictional forces were found to have minimal effects on the forming pressure; as most of the deformation takes place in the free part of the sheet. On the other hand, when the sheet touches the die bottom surface and the sidewalls, surface friction at the die-sheet interface restricts the metal flow, resulting in higher forming pressure and prolonged forming time.

5.2 Variable Strain Rate Forming

Based on the stability analysis discussed in section 3, a variable strain rate forming path, shown in Figure 6, is designed in such a way that the ratio of the strain in the local area to that in the uniform area doesn't exceed 1.5. The smooth pressure control algorithm discussed in section 4 is used here to adjust the forming pressure according to the

target strain rate values. The optimal homogenous friction coefficient (μ = 0.4), found in the previous subsection, is applied at the die sheet interface. The thickness distribution obtained with the variable strain rate path along with that obtained using a constant strain rate of 0.01 s-1 are shown in Figure 7, while Figure 8 shows the forming pressure profiles for the two cases.

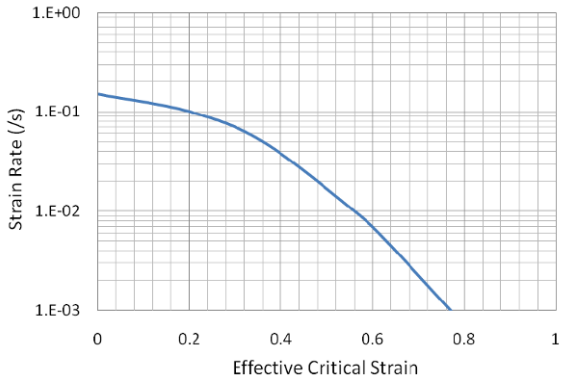

Figure 6: Optimal variable strain rate path.

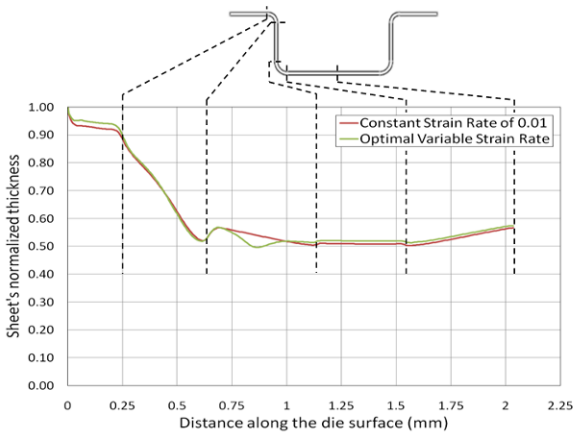

Figure 7: Predicted thickness profile of the formed sheet with constant strain rate of 0.01 s^{-1}, and with the optimal variable strain rate path.

With the variable strain rate path, the forming process is initially carried out at high strain rate values. As the forming process proceeds and more deformation takes place, the edge of instability is approached. Thus, the forming process is slowed down gradually so as to keep the deformation stable, and avoid severe strain localization. With this forming path, it was possible to reduce forming time to 46 seconds, compared to 84 seconds required to form the same part with 0.01 s^{-1} constant strain rate, representing a 45% reduction. Despite of the significant savings in the forming time achieved with the optimal variable strain rate path, the thickness distribution of the formed part is almost comparable with that obtained using the constant strain rate approach.

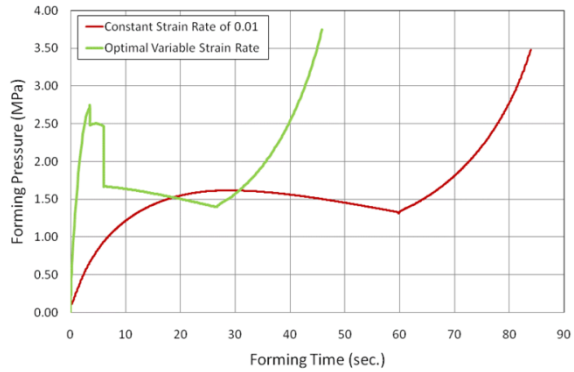

Figure 8: Forming pressure profile for the flow channel formed with constant strain rate of 0.01 s^{-1}, and with the optimal variable strain rate path.

These results show that by carefully designing the forming strain rate path and the friction distribution at the die-sheet interface, significant time savings can be achieved without compromising the integrity of the formed parts.

6 CONCLUSIONS

A nonlinear stability criterion that accounts for geometrical instabilities along with microstructural features has been applied here to design an optimal variable strain rate forming path for a PEMFC bipolar plates' flow channels. The effects of frictional forces acting at the die-sheet interface on the deformation stability were also studied. It was found that larger friction coefficients increase deformation stability, allowing for higher strain rates to be applied.

For the flow channels geometry considered here, a homogeneous friction coefficient of 0.4 was found to be the optimal value. Using this friction coefficient along with the variable strain rate forming path, it was possible to reduce forming time by 45%, without compromising the integrity of the formed part.

References

[1] U.S Department of Transportation, *Transportation Role in Reducing U.S. Greenhouse Gas Emissions*, 2010.

[2] F.K. Abu-Farha and M.K. Khraisheh, "An integrated approach to the Superplastic Forming of lightweight alloys: towards sustainable manufacturing," *International Journal of Sustainable Manufacturing*, vol. 1, 2008, pp. 18–40.

[3] A. Hermann, T. Chaudhuri, and P. Spagnol, "Bipolar plates for PEM fuel cells: A review," *International Journal of Hydrogen Energy*, vol. 30, Sep. 2005, pp. 1297-1302.

[4] D.G. Sanders, "The current state-of-the-art and the future in airframe manufacturing using superplastic forming technologies," *Materials Science Forum*, 2001, pp. 17–22.

[5] M.A. Nazzal, M.K. Khraisheh, and B.M. Darras, "Finite element modeling and optimization of superplastic forming using variable strain rate approach," *Journal of Materials Engineering and Performance*, vol. 13, 2004, pp. 691–699.

[6] M.K. Khraisheh and H.M. Zbib, "Optimum forming

loading paths for Pb-Sn superplastic sheet materials," *Journal of Engineering Materials and Technology*, vol. 121, 1999, p. 341.

[7] L. Carrino, G. Giuliano, and C. Palmieri, "On the optimisation of superplastic forming processes by the finite-element method," *Journal of Materials Processing Technology*, vol. 143, 2003, pp. 373–377.

[8] P.E. Krajewski and J.T. Carter, *Lubrication of magnesium workpieces for hot forming*, Google Patents, 2007.

[9] F.S. Jarrar, F.K. Abu-Farha, L.G. Hector, and M.K. Khraisheh, "Simulation of High-Temperature AA5083 Bulge Forming with a Hardening/Softening Material Model," *Journal of materials engineering and performance*, vol. 18, 2009, pp. 863–870.

[10] M.K. Khraisheh and F.K. Abu-Farha, "Microstructure-Based Modeling of Anisotropic Superplastic Deformation," *TECHNICAL PAPERS-SOCIETY OF MANUFACTURING ENGINEERS-ALL SERIES-*, 2003.

[11] C.H. Caceres and D.S. Wilkinson, "Large strain behaviour of a superplastic copper alloy–I. Deformation," *Acta Metallurgica*, vol. 32, 1984, pp. 415–422.

[12] M.J. Stowell, "Failure of superplastic alloys," *Metal Science*, vol. 17, 1983, pp. 1–11.

[13] Z. Marciniak and K. Kuczynski, "Limit strains in the processes of stretch-forming sheet metal," *International Journal of Mechanical Sciences*, vol. 9, 1967, pp. 609–612.

[14] J.W. Hutchinson, K.W. Neale, and A. Needleman, "Sheet necking—I. Validity of plane stress assumptions of the long-wavelength approximation," *Mechanics of Sheet Metal Forming, Plenum Press, New York*, 1978, pp. 111–126.

[15] Mohammad Albakri and Marwan Khraisheh, "Flow Field Design And Optimization For PEM Fuel Cell Bipolar Plates," 2009.

[16] ABAQUS, *Abaqus Analysis User's Manual*.

[17] S.G. Luckey and P. Friedman, "Aspects of element formulation and strain rate control in the numerical modeling of superplastic forming.," *Advances in Superplasticity and Superplastic Forming as held at the 2004 TMS Annual Meeting*, 2004, pp. 371–380.

[18] F.S. Jarrar, L.G. Hector Jr, M.K. Khraisheh, and A.F. Bower, "New approach to gas pressure profile prediction for high temperature AA5083 sheet forming," *Journal of Materials Processing Technology*, 2010.